Journal of Inflammation Research

Dovepress
Taylor & Francis Group

Open Access Full Text Article

ORIGINAL RESEARCH

Observation of the Effects of Infrapatellar Fat Pad Excision on the Inflammatory Progression of Knee Osteoarthritis in Mice

Ya Li[1,2,*], Peizhi Lu[1,2,*], Haoyu Yao[2], Shuo Yang[2], Bizhi Tu[2], Lingchao Kong[2], Rende Ning[1,2]

[1]Graduate School, Bengbu Medical University, Bengbu, Anhui, People's Republic of China; [2]Department of Orthopedics, The Third Affiliated Hospital of Anhui Medical University, The First People's Hospital of Hefei, Hefei, Anhui, People's Republic of China

*These authors contributed equally to this work

Correspondence: Lingchao Kong, Department of Orthopedics, The Third Affiliated Hospital of Anhui Medical University, The First People's Hospital of Hefei, Hefei, Anhui, People's Republic of China, Tel +86 13956910088, Email konglingchaocn@163.com; Rende Ning, Graduate School, Bengbu Medical University, Bengbu, Anhui, People's Republic of China, Tel +86 13956966305, Email nrd1972@outlook.com

Background: Knee osteoarthritis (KOA) is a degenerative joint disease characterized by cartilage degradation, synovial inflammation, and joint pain. The infrapatellar fat pad (IFP) has been suggested to play a role in modulating the inflammatory processes in KOA. Excision of the IFP is considered a potential therapeutic approach to reduce inflammation and slow disease progression.

Methods: A mouse model of KOA was used to evaluate the impact of IFP excision on inflammation. Mice were divided into five groups: sham (control), unexcised IFP, quarter excision, partial excision, and complete excision of the IFP. Knee joints were collected at early, middle, and late stages of KOA. Gait analysis, micro-computed tomography (micro-CT), HE staining, Safranin O-Fast Green staining, and immunohistochemistry (IHC) were performed to assess joint stability, bone changes, and inflammatory markers (*MMP-3, IL-6, TNF-α, COL-2*). qRT-PCR was conducted for cartilage tissue analysis.

Results: Partial IFP excision significantly improved joint stability, particularly in the middle and late stages of KOA. Micro-CT analysis showed increased bone volume fraction (BV/TV) and trabecular thickness (Tb.Th) in excised groups, with the most significant effects in the partial and complete excision groups. IHC and qRT-PCR indicated reduced *MMP-3, IL-6*, and TNF-α levels in excised groups, particularly in the partial and complete excision groups, suggesting reduced inflammation. *COL-2* expression was higher in excised groups, particularly in late-stage KOA, indicating cartilage protection. The partial excision group exhibited the most balanced reduction in inflammation and improved cartilage integrity across all disease stages.

Conclusion: IFP excision, especially partial excision, significantly modulates the inflammatory response in KOA. Partial excision showed the most effective and balanced impact on joint stability, bone integrity, and cartilage protection, offering potential as a therapeutic approach for KOA.

Keywords: knee osteoarthritis, infrapatellar fat pad, inflammation, micro-CT, mouse model

Introduction

Knee osteoarthritis (KOA) is a common chronic joint disease characterized by the degradation of articular cartilage, osteophyte formation, and inflammation around the joints.[1] Although KOA has traditionally been considered a disease of the elderly, its prevalence has gradually increased in recent years due to population aging and changes in lifestyle, imposing a serious burden on human health.[2] The main risk factors for KOA include aging (which leads to cartilage degradation and reduced regenerative capacity),[3] obesity (which increases joint loading and promotes metabolic inflammation),[4,5] genetic predisposition (which affects cartilage and bone metabolism),[6] biomechanical abnormalities (such as joint malalignment and previous injuries),[7] and chronic inflammation (which accelerates joint degradation through pro-inflammatory mediators).[6] KOA is now recognized as a complex disorder affecting the entire joint, involving not only articular cartilage and subchondral bone but also the synovial membrane, menisci, tendons, ligaments, and the

Received: 13 January 2025
Accepted: 30 April 2025
Published: 23 May 2025

infrapatellar fat pad (IFP).[8,9] The pathological changes in KOA go beyond cartilage degradation, involving synovial inflammation, meniscal degeneration, ligament dysfunction, and structural alterations in the IFP.[10]

The IFP, located beneath the patella in the knee joint, is an important structure that plays a crucial role in maintaining joint stability, reducing friction, and regulating joint physiological activities.[11–13] However, in KOA, the IFP undergoes pathological changes, including fibrosis, volume reduction, and increased inflammatory cytokine production, which contribute to disease progression.[10] As a key source of inflammatory mediators, the IFP interacts with the synovial membrane, exacerbating synovial inflammation and joint destruction.[14]

The management of the IFP in clinical practice remains a subject of debate. Under physiological conditions, the IFP plays a critical role in maintaining joint stability, providing mechanical cushioning, and regulating immune responses. However, during inflammation, the IFP can act as a significant source of pro-inflammatory mediators, thereby exacerbating the inflammatory process.[15–17] Previous studies have demonstrated that complete excision of the IFP can alleviate inflammation to some extent.[18] Nevertheless, given the essential physiological functions of the IFP, total removal may also have adverse effects on joint function.[19] To date, research investigating the impact of IFP excision on inflammation and joint integrity remains limited.

By employing a multi-faceted approach, this study systematically evaluated the impact of varying degrees of IFP removal on joint inflammation. Our aims to elucidate how different extents of IFP excision influence KOA progression, providing valuable scientific insights and guidance for clinical treatment strategies.

Materials and Methods

This study systematically investigates the effects of different IFP excision strategies on the progression of KOA using a mouse model. The experimental design includes groups with complete IFP excision, one-quarter excision, partial excision, and unexcision, with observations spanning the early, middle, and late stages of inflammation.

Experimental Overview

One hundred and fifty male C57BL/6 mice, aged 6 to 8 weeks and weighing approximately 20 grams, were randomly divided into five groups (30 mice per group). The groups were as follows:

Control Group

Mice underwent sham surgery only.

Unexcised Group

The IFP was left intact, and the KOA model was induced without excision of the IFP.

Quarter Excision Group

Approximately one-quarter of the IFP was excised while inducing the KOA model.

Partial Excision Group

Approximately half of the IFP was excised while inducing the KOA model.

Complete Excision Group

The entire IFP was excised while inducing the KOA model.

All mice underwent a one-week acclimatization period before the IFP excision surgeries. Mice were euthanized at 4 weeks (early OA), 8 weeks (mid-stage OA), and 12 weeks (late-stage OA)[20] (Figure 1A) After euthanasia, the joints were flushed with 100 μL of sterile saline (Yuanye China Cat no: R41102). Half of the knee joint samples were stored in liquid nitrogen, while the other half were fixed in 4% formaldehyde (Aladdin China Cat no: P395744) for 48 hours.

Surgical Removal of the IFP

The KOA mouse model was established using the modified Hulth method.[21] The day before modeling, mice are fasted for 12 hours. Zoletil 50 (Virbac USA Cat no: ZOLE50) is diluted at a ratio of 1 to 10. The weight of each mouse is recorded to calculate the injection dose (10 μL/1 g). The mice are then anesthetized via intraperitoneal injection.

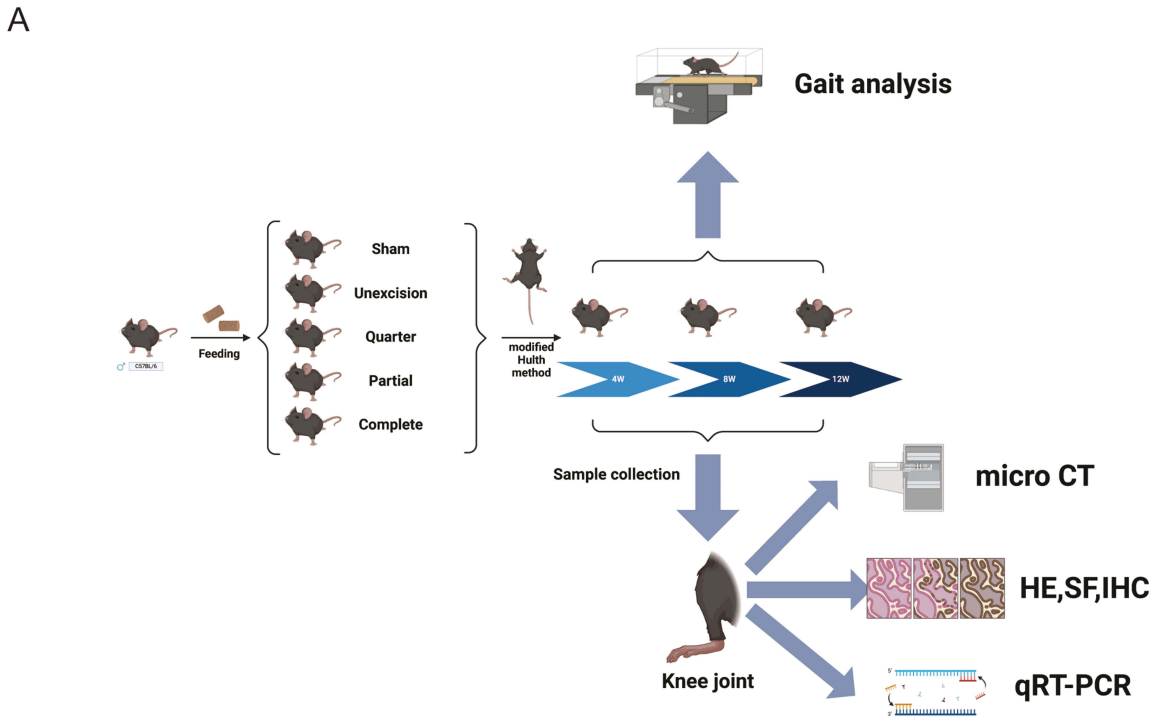

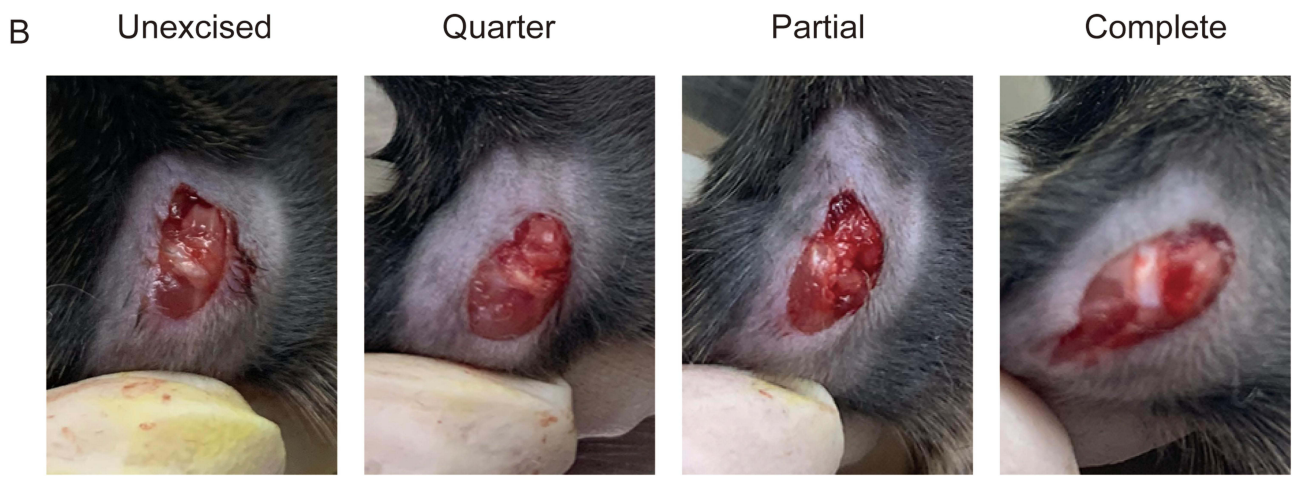

Figure 1 Experimental workflow and mouse modeling images. (**A**) The entire experimental workflow, including mouse breeding, grouping, model establishment, tissue collection, and validation. (**B**) From left to right: mice with no IFP excision, Quarter IFP excision, Partial IFP excision, and Complete IFP excision.

Following anesthesia, the mice are placed on an operating table, and the hair on the right hind limb knee joint area is shaved off using a clipper. The knee joint area is disinfected with an alcohol swab. A sterile surgical blade is used to gently incise the lateral skin and muscle tissue to expose the inner structures. The medial collateral ligament is located and severed, opening the entire joint cavity.

The anterior and posterior cruciate ligaments and the medial meniscus are then cut. A drawer test is performed to confirm the complete rupture of the cruciate ligaments. Corresponding volumes of the IFP are also excised (Figure 1B). Hemostasis is achieved, and the incisions are sutured layer by layer using surgical sutures.

https://doi.org/10.2147/JIR.S517314

Gait Assessments

A mandatory treadmill based gait analysis was performed on half of all animals (N = 75) using VisuGait Gait analysis system (Shanghai Xinsoft Information Technology Co, Shanghai, China).[22] To ensure consistency and reduce stress, the animals acclimated to the system over the course of a week, during which they were introduced to the treadmill environment and allowed to familiarize themselves with the device. Data collection is carried out by the same trained handlers to reduce variability, and all records are taken within the same time window (5pm to 12pm) to reduce the diurnal effects of animal behaviour. The order of the animals analyzed was random to avoid potential sequential effects and to ensure that the data collected was representative and unbiased.[23]

Tissue Collection

All animals were collected at early, middle, and late stages as per the experimental design. At the time of collection, each animal's body weight was recorded. The animals were then humanely euthanized in a CO_2 chamber to ensure a painless and ethical process.[24] Following euthanasia, the hind limbs were carefully dissected at the hip joint. Both left and right hind limbs were removed; six mice had their knee joints immediately snap-frozen in liquid nitrogen, while the remaining four mice had their knee joints fixed in 10% neutral buffered formalin (Yuanye China Cat no: R22054) for 48 hours.

After fixation, the limbs were transferred to phosphate-buffered saline (PBS) (Acmec, China, Cat no: AC13319) for subsequent processing and micro-computed tomography (micro-CT) analysis.

Following micro-CT imaging and bone grading, the limbs were decalcified in ethylenediaminetetraacetic acid (EDTA) (Aladdin, China, Cat no: A301488) solution (pH 5.5). The EDTA solution was refreshed every two days for a duration of four weeks to ensure complete decalcification of the bone tissue, enabling downstream histological analysis.[25]

MicroCT

Micro-computed tomography (micro CT) (Tianjin Sanying Precision Instrument Co, Tianjin, China) was employed to quantitatively analyze bone parameters, providing high-resolution 3D imaging of the trabecular bone structure. Scans were performed using a microCT system (micro CTA), and image data were reconstructed and analyzed with Dragonfly software (Object Research Systems (ORS) Inc. Montreal, Quebec, Canada). Key trabecular bone measurements included the bone volume to tissue volume ratio (BV/TV), trabecular thickness (Tb.Th), and trabecular separation (Tb.Sp). These parameters were assessed to evaluate bone microarchitecture and density, enabling detailed comparisons across experimental groups and stages of KOA.[26,27]

Histologic Grading of OA

After micro-CT analysis, knee joint samples were decalcified in EDTA, fixed in 4% formaldehyde for 48 hours, dehydrated in graded ethanol, and embedded in paraffin. Tissue sections (~5 μm thick) were prepared for histological analysis to assess the effects of IFP excision on KOA progression.

HE staining was used to evaluate synovial inflammation and cartilage structural changes. Sections were deparaffinized, rehydrated, stained with hematoxylin (Acmec, China, Cat no: 517-28-2) for 5 minutes, differentiated in 1% acid alcohol (Meryer, China, Cat no: 64-17-7), counterstained with 0.5% eosin (Yuanye, China, Cat no: R30114) for 1–2 minutes, dehydrated, and mounted. Microscopic analysis was performed to assess inflammation and cartilage structure.[28,29]

Safranin O/Fast Green staining assessed cartilage matrix degradation and structural changes in cartilage and bone. Sections were deparaffinized, stained with Fast Green (0.5%) (Yuanye, China, Cat no: R20751) for 5 minutes, washed with 1% acetic acid, then stained with Safranin O (0.1%) (Yuanye, China, Cat no: R22045) for 5 minutes.[30] After dehydration and mounting, cartilage degeneration was analyzed microscopically and scored using the Osteoarthritis Research Society International (OARSI) system.[31,32] A score of 0 represents normal cartilage, while a score of 0.5 indicates loss of Safranin-O staining without structural changes. A score of 1 corresponds to small fibrillations without loss of cartilage. A score of 2 is assigned when vertical clefts extend down to the layer immediately below the superficial

layer, with some loss of surface lamina. Scores of 3 to 6 represent increasing severity of cartilage damage, with vertical clefts or erosion extending to the calcified cartilage and varying percentages of the articular surface affected. Specifically, a score of 3 indicates vertical clefts or erosion extending to less than 25% of the articular surface, while a score of 4 corresponds to extension to 25–50%. A score of 5 reflects clefts or erosion extending to 50–75% of the articular surface, and a score of 6 is given when the clefts or erosion extend to more than 75% of the articular surface. These scores provide a comprehensive assessment of cartilage degeneration in KOA.[33]

IHC and Quantitative Analysis

To evaluate the effects of IFP excision on inflammatory progression and cartilage degeneration in KOA, IHC staining was performed for matrix metalloproteinase-3 (*MMP-3*), interleukin-6 (*IL-6*), tumor necrosis factor-alpha (*TNF-α*), and type II collagen (*Col-2*).[34]

Knee joint samples were fixed in 4% paraformaldehyde, dehydrated in graded ethanol, embedded in paraffin, and sectioned (5 μm). After deparaffinization, rehydration, and antigen retrieval in sodium citrate buffer (pH 6.0) (Aladdin, China, Cat no: P299403) at 95°C, sections were blocked with 10% goat serum. They were incubated overnight at 4°C with primary antibodies: anti-*MMP-3* (Abcam, UK, Cat no: ab53015), anti-*IL-6* (Abcam, UK, Cat no: ab6672), anti-*TNF-α* (Abcam, UK, Cat no: ab6671), anti-*Col-2* (Abcam, UK, Cat no: ab34712), and then with a biotinylated secondary antibody for 1 hour at room temperature.

Staining was visualized using DAB (Aladdin, China, Cat no: D405772) as the chromogen, and nuclei were counterstained with hematoxylin. Sections were dehydrated, cleared, and mounted. Microscopic images were captured, and the expression levels of *MMP-3, IL-6, TNF-α*, and *Col-2* were quantified and compared to controls.

qRT-PCR (Quantitative Reverse Transcription PCR) Analysis

The knee joint cartilage tissue stored in liquid nitrogen is retrieved and immediately ground into a powder under low-temperature conditions using a liquid nitrogen grinding mill to ensure RNA integrity.[35] The powdered tissue is quickly transferred into a centrifuge tube containing Trizol (Yuanye, China, Cat no: R21086) reagent and thoroughly homogenized to lyse the cells and release RNA.[36] Following the protocol of Trizol reagent, chloroform (Aladdin, China, Cat no: C434285) is added for phase separation, and the aqueous phase containing total RNA is collected after centrifugation. The aqueous phase is then transferred to a new tube, and RNA is precipitated using isopropanol (Aladdin, China, Cat no: I141145). After washing to remove impurities, the RNA is dissolved in RNase-free water to obtain pure RNA samples. The purity and concentration of RNA are measured using a spectrophotometer (Mapada, Shanghai, China) to ensure suitability for downstream experiments. Subsequently, the extracted RNA is reverse transcribed into cDNA using a reverse transcription kit (Yeasen, Shanghai, China). In the qRT-PCR reaction system, the cDNA template, specific primers, and fluorescent dye are combined, and the optimized program is run on a real-time PCR machine to perform amplification reactions. The final output provides the expression levels of target genes. Primers are shown in (Table 1).

Table 1 Primer Sequences of Target Genes

Gene	Forward Primer	Reverse Primer
TNF-α	5′-CATCTTCTCAAAATTCGAGTGACAA-3′	5′-TGGAGTAGACAAGGTACACACC-3′
IL-6	5′AAATTCGGTACATCCTCGACGGCA-3′	5′-AGTGCCTCTTTGCTGCTTTCACAC-3′
COL2A1	5′- TCTGTGAAGACACCAAGGACTG −3′	5′- TTCTCCTTTCTGCCCCTTTGGT −3′
MMP3	5′-GATGGAGCTGCAAGGGGTGA-3′	5′-TTCGGGATGCCAGGAAAGG-3′
SOX-9	5′- AAGCTCTGGAGACTGCTGAA −3′	5′- CCCATTCTTCACCGACTTCCT −3′
ADAMTS-5	5′- ATGCAGCCATCCTGTTCAC −3′	5′- CATTCCCAGGGTGTCACAT −3′
GAPDH	5′-GATGATTGGCATGGCTTT-3′	5′-CACCTTCCGTTCCAGTTT-3′

Abbreviations: TNF-α, tumor necrosis factor-alpha; IL-6, interleukin-6; COL2A1, collagen type II alpha 1 chain; MMP3, matrix metalloproteinase-3; SOX-9, SRY-box transcription factor 9; ADAMTS-5, a disintegrin and metalloproteinase with thrombospondin motifs 5; GAPDH, glyceraldehyde-3-phosphate dehydrogenase.

Statistical Analyses

Before comparing data, tests for homogeneity of variance, independence, and normality will be conducted. If these assumptions are satisfied, Student's *t*-test will be used for comparisons; otherwise, the rank-sum test will be applied. All statistical analyses were performed using GraphPad Prism 9.5 software. All results were expressed as mean ± standard deviation (mean ± SEM). Statistical analysis was performed to compare differences between groups, with a P-value <0.05 considered statistically significant.

Results

Gait Analysis Reveals That the Overall Joint Stability in the Excision Group Is Superior to That in the Unexcision Group, with the Most Significant Improvement Observed in the Partial Excision Group

All mice underwent gait acclimation training one week prior to tissue collection to ensure stable and consistent walking for gait analysis. Gait assessment and data collection were conducted the day before tissue collection.[37,38] The movement trajectory of mice with complete IFP excision was recorded (Figure 2A). At the 4-week stage, the left stride length (Figure 2B), right stride length (Figure 2C), forelimb stride width (Figure 2D), and hindlimb stride width (Figure 2E) were measured for all experimental groups. At the 8-week stage, the left stride length (Figure 2F), right stride length (Figure 2G), forelimb stride width (Figure 2H), and hindlimb stride width (Figure 2I) were measured. Similarly, at the 12-week stage, these same parameters were assessed (Figure 2J–M). Statistical analysis revealed a compensatory increase in left stride width in KOA mice at all stages (4, 8, and 12 weeks). The partial excision group showed significant improvement at 8 weeks ($P < 0.01$) and at 12 weeks compared to the complete and quarter excision groups ($P < 0.001$, $P < 0.05$). The complete excision group also reduced the difference compared to the unexcision group at 12 weeks ($P < 0.05$).

For right stride width, partial excision consistently improved performance at all time points. The quarter excision group showed improvement at 12 weeks ($P < 0.05$), while the complete excision group improved only at 4 weeks ($P < 0.01$).

No significant differences were found in forelimb stride width across groups. However, for hindlimb stride width, partial excision showed significant improvement at 8 and 12 weeks. The complete excision group showed improvement at 8 weeks ($P < 0.05$) and both quarter and complete excision groups showed significant improvement at 12 weeks ($P < 0.01$, $P < 0.001$).

In conclusion, the partial excision group most effectively maintained joint stability, while all excision groups improved hindlimb stride width compared to the non-resected group.

Partial Excision of the IFP Significantly Improves Joint Damage Throughout the Early, Middle, and Late Stages of KOA, While Complete Excision Also Offers a Certain Degree of Therapeutic Benefit

Three-dimensional reconstruction of the knee joints in all mice revealed significantly reduced osteophyte formation in the excision groups compared to the unexcision group (Figure 3A). Quantitative analysis at 4 weeks showed a significant reduction in Tb.Sp in the partial excision group compared to the unexcision group ($P < 0.05$), while no significant differences were observed among the groups in Tb.N, Tb.Th, and BV/TV (Figure 3B–E).

At 8 weeks, all excision groups outperformed the unexcision group. Specifically, both the partial and complete excision groups showed significantly higher Tb. N and lower Tb. Sp values compared to the unexcision group ($P < 0.01$, $P < 0.05$). In terms of Tb.Th, the quarter excision group demonstrated a significant increase compared to the unexcision group ($P < 0.05$), while both the partial and complete excision groups showed even greater increases ($P < 0.001$, $P < 0.01$). For BV/TV, the partial excision group exhibited significantly higher values than both the unexcision and quarter excision groups ($P < 0.05$) (Figure 3F–I).

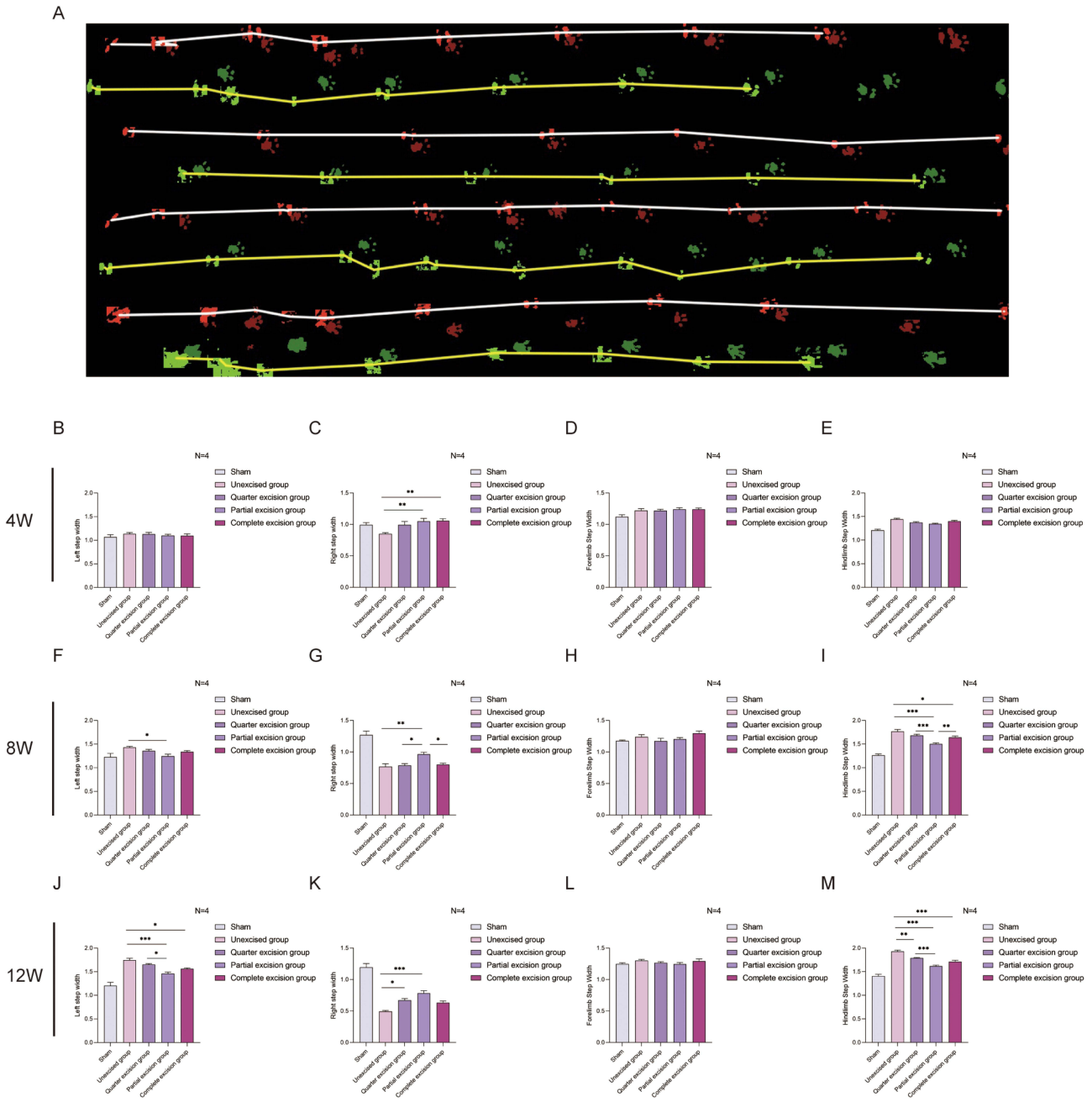

Figure 2 Mouse gait trajectory maps and gait experiment analysis results: (**A**) From top to bottom, the movement trajectory maps of normal mice and IFP full-excision mice at 4,8,12 weeks. (**B**) The left stride length of all experimental mice at the 4 weeks. (**C**) The right stride length of all experimental mice at the 4 weeks. (**D**) The forelimb stride width of all experimental mice at the 4 weeks. (**E**) The hindlimb stride width of all experimental mice at the 4 weeks. (**F**) The left stride length of all experimental mice at the 8 weeks. (**G**) The right stride length of all experimental mice at the 8 weeks. (**H**) The forelimb stride width of all experimental mice at the 8 weeks. (**I**) The hindlimb stride width of all experimental mice at 8 weeks. (**J**) The left stride length of all experimental mice at the 12 weeks. (**K**) The right stride length of all experimental mice at the 12 weeks. (**L**) The forelimb stride width of all experimental mice at the 12 weeks. (**M**) The hindlimb stride width of all experimental mice at the 12 weeks. N=5. All the data in the bar graph are presented as mean ± S.E.M, among which, *P < 0.05, **P < 0.01, and ***P < 0.001.

At 12 weeks, Tb. N in the partial excision group was significantly higher than in both the unexcision and quarter excision groups ($P < 0.001$, $P < 0.05$), and also significantly higher in the complete excision group compared to the unexcision group ($P < 0.05$). Regarding Tb.Sp, the partial excision group showed significantly lower values than all other groups ($P < 0.01$, $P < 0.05$, $P < 0.05$). For Tb.Th, the partial excision group again exhibited significantly higher values than the other three groups ($P < 0.001$ for all comparisons), and the complete excision group also showed a significant increase compared to the unexcision group ($P < 0.01$). Finally, in terms of BV/TV, the partial excision group

https://doi.org/10.2147/JIR.S517314

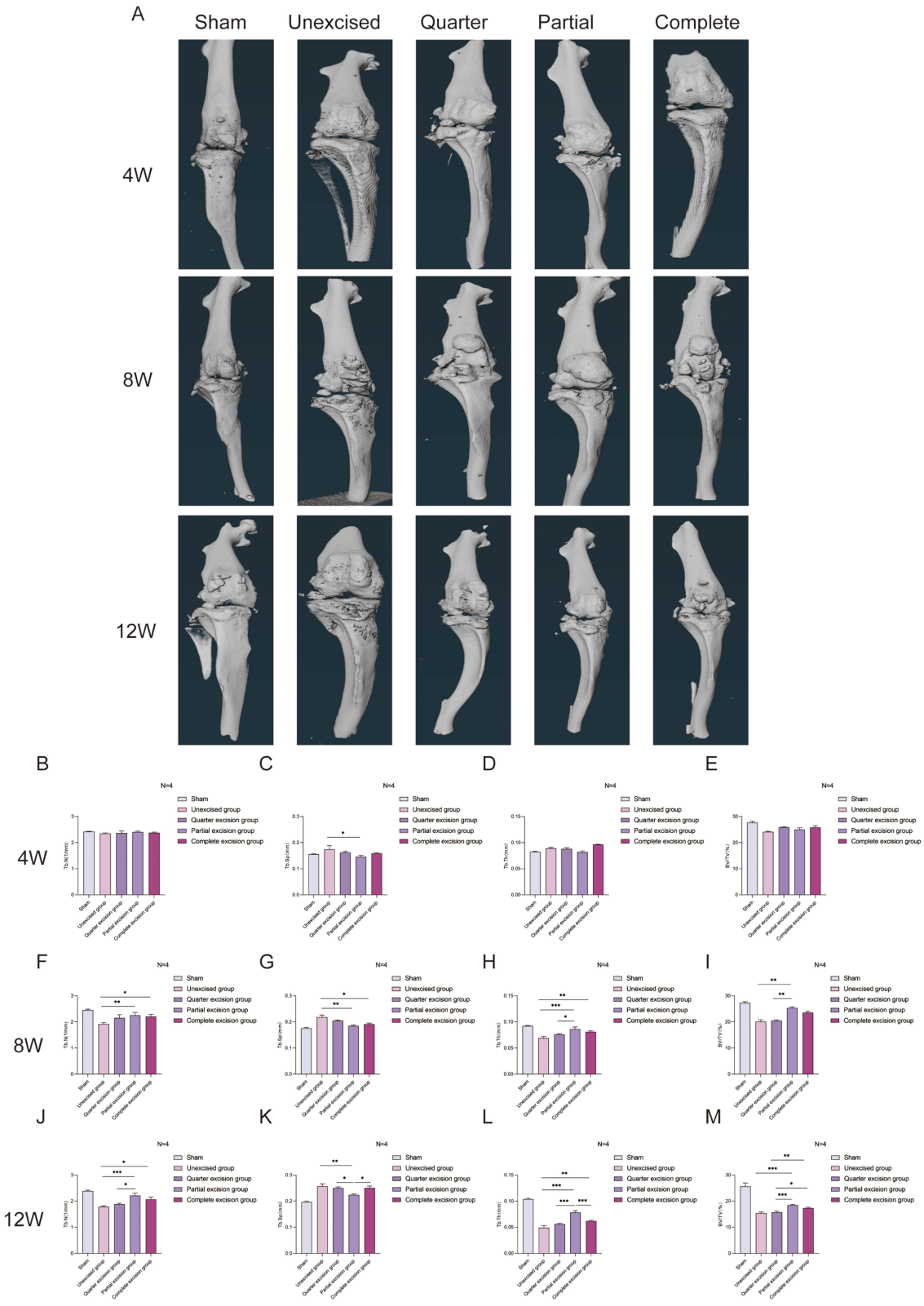

Figure 3 Mouse knee joint images under micro-CT and micro-CT experimental analysis results: (**A**) Knee joint images under different grouping conditions at 4,8,12 weeks. (**B**) Tb.N of all experimental mice at the 4 weeks. (**C**) Tb.Sp of all experimental mice at the 4 weeks. (**D**) Tb.Th of all experimental mice at the 4 weeks. (**E**) BV/TV of all experimental mice at the 4 weeks. (**F**) Tb.N of all experimental mice at the 8 weeks. (**G**) Tb.Sp of all experimental mice at the 8 weeks. (**H**) Tb.Th of all experimental mice at the 8 weeks. (**I**) BV/TV of all experimental mice at the 8 weeks. (**J**) Tb.N of all experimental mice at the 12 weeks. (**K**) Tb.Sp of all experimental mice at the 12 weeks. (**L**) Tb. Th of all experimental mice at the 12 weeks. (**M**) BV/TV of all experimental mice at the 12 weeks. N=4. All the data in the bar graph are presented as mean ± S.E.M, among which *P < 0.05, **P < 0.01, and ***P < 0.001.

demonstrated significantly higher values compared to both the unexcision and quarter excision groups ($P < 0.001$), and the complete excision group also showed significantly higher values than the unexcision and quarter excision groups ($P < 0.01$, $P < 0.05$) (Figure 3J–M).

In conclusion, the partial excision group most effectively preserved bone structure and remodeling balance, improving KOA progression. Both the partial and complete excision groups showed significant benefits compared to the unexcision group.

Histologic Grading of OA: HE Staining, Safranin O-Fast Green Staining, and OARSI Score Analysis of Cartilage Damage

HE staining of knee joint sections revealed significant histological changes as KOA progressed. In the healthy state, the cartilage surface was smooth, with intact layers and orderly arranged chondrocytes. At 4 weeks, mild roughness and slight fissures appeared, with some chondrocyte clustering. By 8 weeks, the cartilage showed increased fissuring and thinning of trabeculae, with reduced chondrocyte numbers. At 12 weeks, large cartilage defects were evident, with exposed subchondral bone, trabecular sclerosis, and matrix loss. Notably, the partial and complete excision groups exhibited better histological outcomes than the unexcision group (Figure 4A).

Safranin O-Fast Green staining showed reduced proteoglycan content by 4 weeks, with significant loss and cartilage degradation by 12 weeks. The partial excision group retained more proteoglycan staining compared to other groups, indicating less severe degradation (Figure 4B).

The OARSI scoring system is a widely used method for evaluating cartilage damage in KOA. It scores cartilage degeneration based on the extent and depth of damage, ranging from normal cartilage to full-thickness loss with exposure of the subchondral bone. OARSI scores at 4, 8, and 12 weeks showed significant improvements in the partial and complete excision groups compared to the unexcision group ($P < 0.001$, $P < 0.05$) at 4 weeks. At 8 weeks, the partial excision group showed significantly lower scores than the quarter excision group ($P < 0.01$). The quarter excision group showed less improvement over time (Figure 4C–E).

In conclusion, the partial excision group demonstrated the best outcomes, with significantly less cartilage degradation and better joint stability than the other groups.

IHC Results: Immunohistochemical Analysis of Inflammatory and Cartilage Markers in KOA Mice

COL-2 immunohistochemistry revealed that at 4 weeks, the partial excision group had significantly higher expression compared to the other groups ($P < 0.001$, $P < 0.05$, $P < 0.01$). At 8 weeks, the partial excision group maintained significantly higher expression than all other groups ($P < 0.001$), and at 12 weeks, it remained significantly higher compared to both the unexcision and quarter excision groups ($P < 0.001$) (Figure 5A).

For *IL-6*, the partial excision group showed the greatest reduction at 4 weeks ($P < 0.01$), and at 8 weeks, it exhibited significantly lower levels than the other excision groups ($P < 0.05$, $P < 0.01$). By 12 weeks, the partial excision group consistently showed the lowest IL-6 levels compared to the unexcision group ($P < 0.05$, $P < 0.001$) (Figure 5B).

MMP-3 results showed that the partial excision group had significantly lower expression at 4, 8, and 12 weeks compared to the other three groups ($P < 0.01$, $P < 0.001$, $P < 0.001$). Both the complete and quarter excision groups also showed reduced expression at mid and late stages compared to the unexcision group (Figure 6A).

TNF-α results revealed that at 8 weeks, all three excision groups had significantly lower expression than the unexcision group. At 12 weeks, the partial excision group exhibited significantly lower expression than the other three groups ($P < 0.001$), while both the quarter and complete excision groups also showed significantly lower expression than the unexcision group (Figure 6B).

The partial excision group showed lower inflammation expression compared to the unexcision group. At 8 and 12 weeks, both the quarter and complete excision groups also demonstrated reduced inflammation compared to the unexcision group, indicating that all excision groups performed better than the unexcision group.

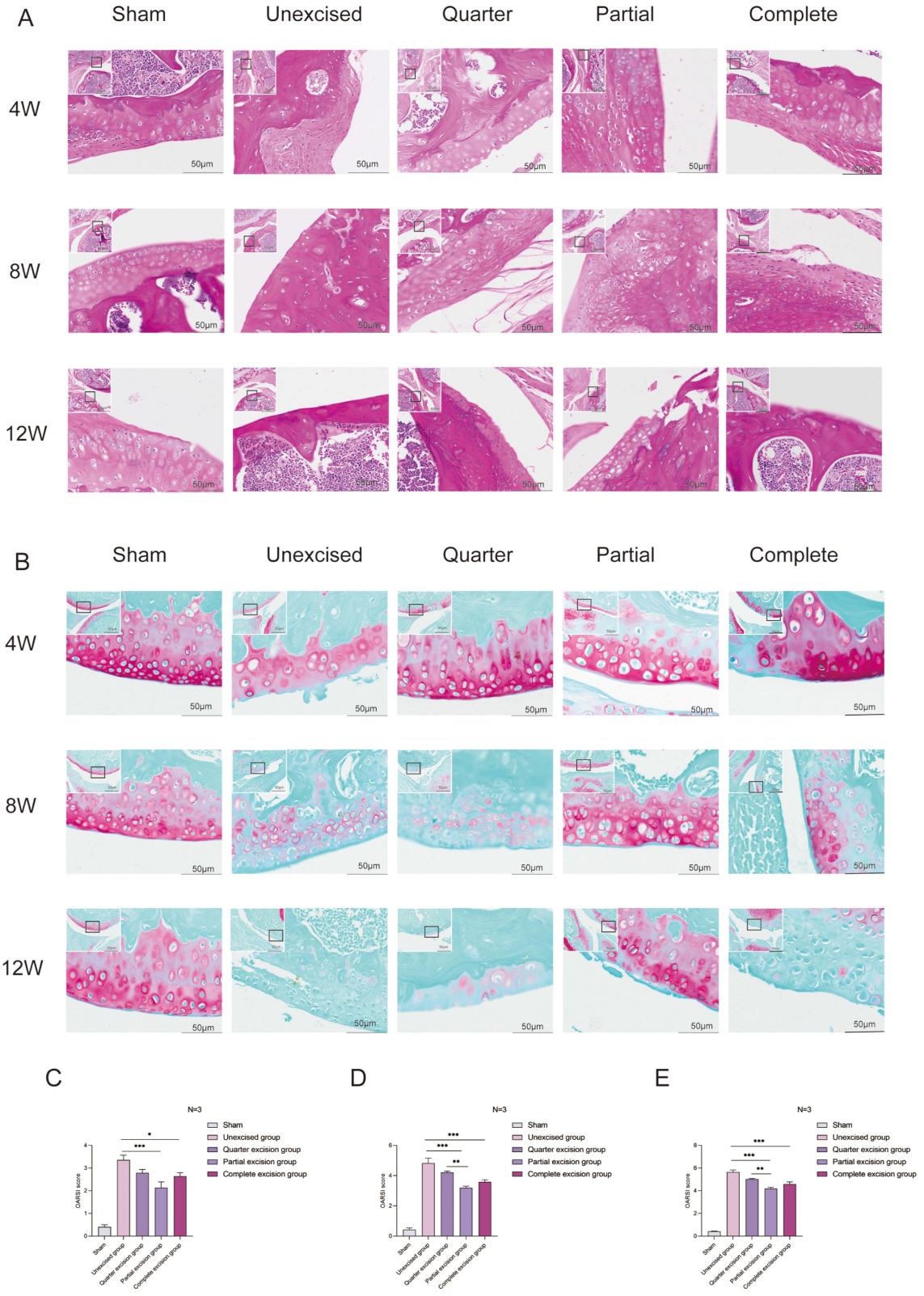

Figure 4 Mouse knee joint HE staining, Safranin O-Fast Green staining, and OARSI scores: (**A**) HE staining of the mouse knee joint, with the scale bar in the top left image at 200 μm and the scale bar in the bottom right image at 400 μm. (**B**) Safranin O-Fast Green staining of the mouse knee joint, with the scale bar in the top left image at 200 μm and the scale bar in the bottom right image at 400 μm. (**C**) OARSI scores of experimental mice at the 4 weeks. (**D**) OARSI scores of mice at the 8 weeks. (**E**) OARSI scores of mice at the 12 weeks. N=3. All the data in the bar graph are presented as mean ± S.E.M, among which *P < 0.05, **P < 0.01, and ***P < 0.001.

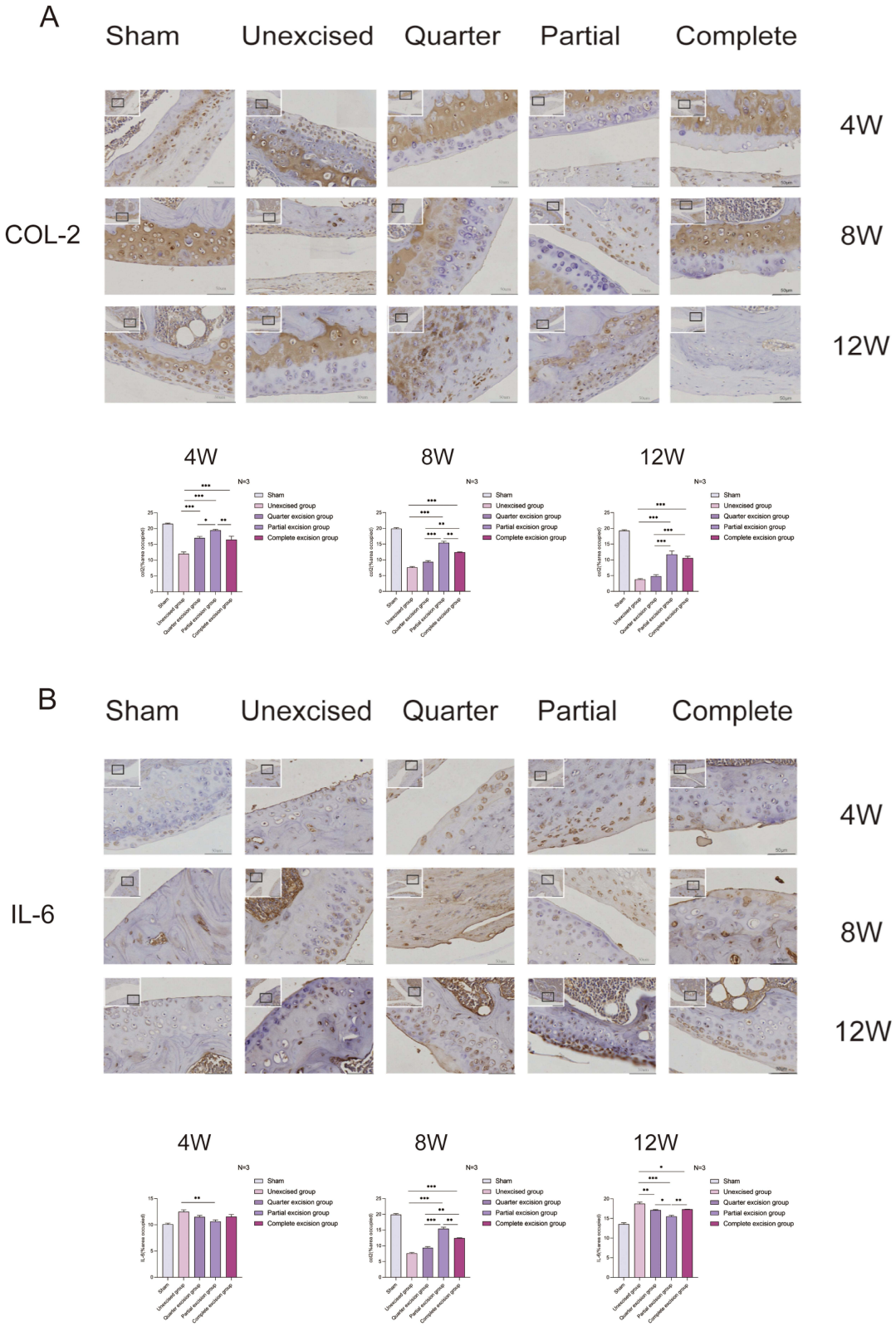

Figure 5 Immunohistochemistry results and quantitative analysis of mouse knee joints: (**A**) COL-2 staining and quantitative analysis of mice at 4,8,12 weeks, with the scale bar in the top left corner at 200 μm and the bottom right corner at 300 μm. (**B**) IL-6 staining and quantitative analysis of mice at 4,8,12 weeks, with the scale bar in the top left corner at 200 μm and the bottom right corner at 300 μm. N=3. All the data in the bar graph are presented as mean ± S.E.M, among which *P < 0.05, **P < 0.01, and ***P< 0.001.

https://doi.org/10.2147/JIR.S517314

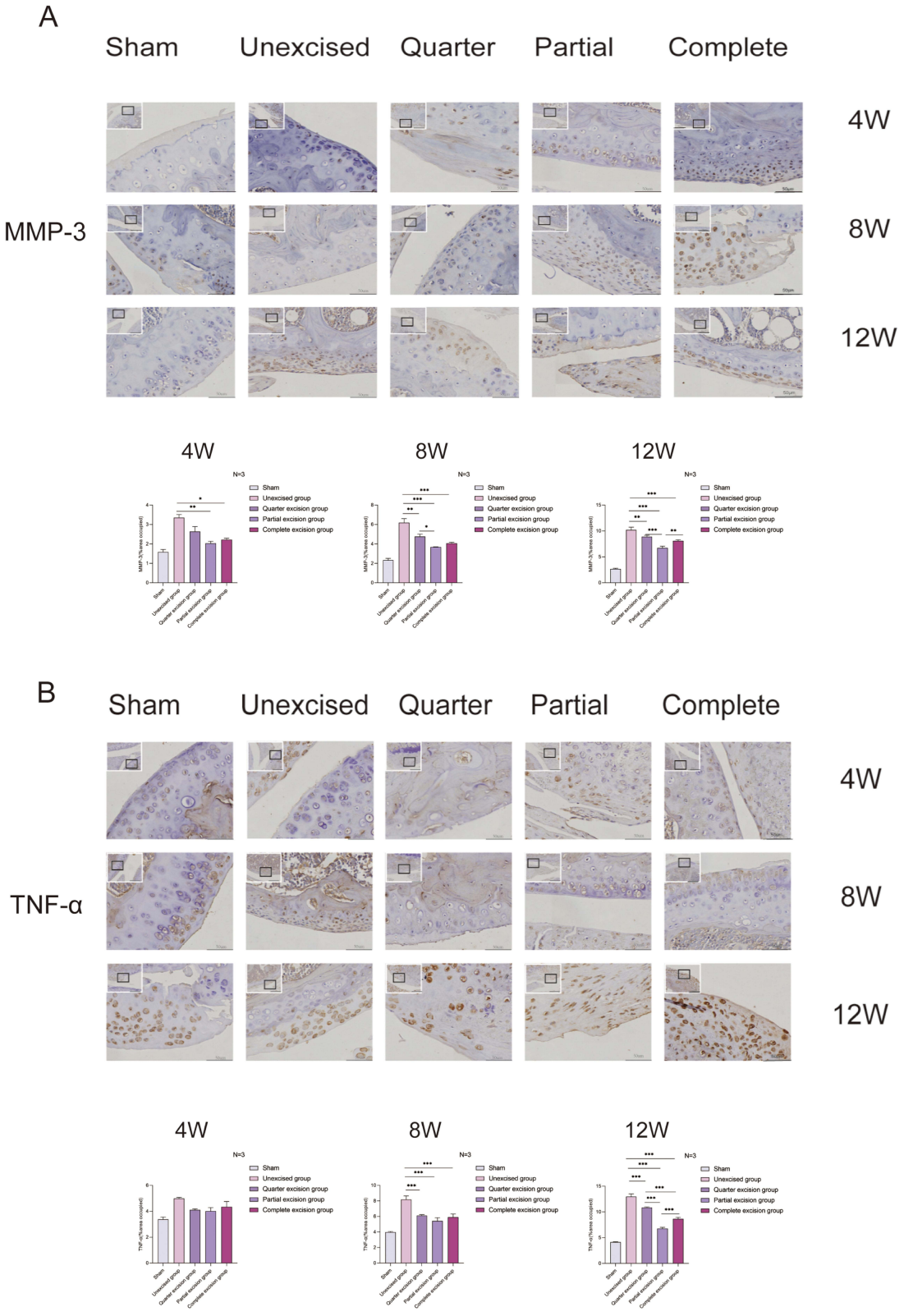

Figure 6 Immunohistochemistry results and quantitative analysis of mouse knee joints: (**A**) MMP-3 staining and quantitative analysis of mice at 4,8,12 weeks, with the scale bar in the top left corner at 200 μm and the bottom right corner at 300 μm. (**B**) TNF-α staining and quantitative analysis of mice at 4,8,12 weeks, with the scale bar in the top left corner at 200 μm and the bottom right corner at 300 μm. N=3. All the data in the bar graph are presented as mean ± S.E.M, among which *P < 0.05, **P < 0.01, and ***P< 0.001.

qRT-PCR Results: Expression of Key Inflammatory, Cartilage, and Matrix Degradation Markers in KOA Mice

At 4 weeks, the partial excision group showed significantly higher *COL2A1* and SRY-box transcription factor 9(*SOX9)* expression ($P < 0.05$), and significantly lower A Disintegrin And Metalloproteinase with Thrombospondin Motifs 5 (*ADAMTS5)* ($P < 0.001$), TNF-α ($P < 0.001$, $P < 0.05$), compared to other groups. *MMP-3* expression was higher in both the partial excision ($P < 0.001$) and complete excision ($P < 0.01$) groups, while IL-6 was slightly reduced but not statistically significant (Figure 7A).

At 8 weeks, the partial excision group exhibited significantly higher *COL2A1* ($P < 0.001$, $P<0.01$), and *SOX9* ($P < 0.001$, $P < 0.05$) expression, and significantly lower *ADAMTS5* ($P < 0.001$), *TNF-α* ($P < 0.001$, $P < 0.01$, $P < 0.01$), *MMP-3* ($P < 0.001$), and *IL-6* ($P < 0.001$) levels compared to the unexcision and quarter excision groups. The complete excision group also showed significant improvements in these markers ($P < 0.01$) (Figure 7B).

At 12 weeks, the partial excision group showed the highest *COL2A1* ($P < 0.001$, $P < 0.01$) and *SOX9* ($P < 0.001$, $P < 0.05$) levels, with significantly lower *ADAMTS5* ($P < 0.001$), *TNF-α* ($P < 0.001$, $P < 0.01$, $P < 0.001$), *MMP-3* ($P < 0.001$, $P < 0.001$, $P < 0.01$), and *IL-6* ($P < 0.001$, $P < 0.05$) expression compared to all other groups. The complete excision group also demonstrated significant reductions in inflammation markers ($P < 0.001$) and better cartilage protection compared to the unexcision and quarter excision groups (Figure 7C).

The partial excision group consistently showed the most favorable outcomes, with significant improvements in *COL2A1, SOX9*, and reductions in *ADAMTS5, TNF-α, MMP-3*, and *IL-6* expression at 4, 8, and 12 weeks, outperforming the other experimental groups.

Discussion

KOA is one of the most prevalent degenerative joint diseases, with its incidence continuously increasing due to the aging population, significantly impairing patients' quality of life.[39] The pathological features of KOA include cartilage degeneration, synovial inflammation, meniscal degeneration, ligament dysfunction, and structural alterations of the IFP.[10,39] Despite current treatment options such as pharmacological therapies, physical interventions, and surgical approaches, there is a lack of effective, long-lasting treatments.[40,41]

IFP has emerged as a critical tissue within the knee joint in recent years. IFP not only plays an essential role in shock absorption and lubrication but also contributes significantly to inflammation, bone metabolism, and cartilage protection.[42] Previous studies have indicated that IFP hypertrophy, inflammation, and its association with joint degenerative changes may be key mechanisms in the onset and progression of KOA.[43–45] It has been proposed that complete excision of IFP may effectively alleviate joint inflammation in animals, thereby slowing the progression of KOA.[18] However, there is limited research on the optimal amount of excision required to effectively reduce inflammation while preserving the normal physiological function of the IFP.

This study aims to explore the effects of different degrees of IFP excision (quarter, partial, and complete excision) in a mouse model of KOA. Using gait analysis, micro-CT, histological assessments (HE and Safranin O-Fast Green staining), OARSI scores, immunohistochemistry, and qRT-PCR, we comprehensively evaluate the therapeutic potential of IFP excision at different stages of KOA.

Gait analysis at 4 weeks showed no significant differences, except for a higher right-side stride base in the partial excision group compared to the complete excision group. At 8 and 12 weeks, the partial excision group had significantly reduced hind limb stride width and a higher stride base, indicating improved joint stability and function. The complete excision group showed some improvement, but less pronounced than the partial excision group, while the quarter excision and unexcision groups showed minimal changes. These results suggest that partial IFP excision is the most effective approach for maintaining joint stability and improving function in KOA.

The IFP plays a dual role in KOA pathogenesis. While it contributes to joint inflammation through secretion of pro-inflammatory cytokines and adipokines (IL-6, leptin), it also provides mechanical protection and lubrication.[46] Structural changes in the joint, particularly alterations in bone and cartilage, are crucial indicators of KOA progression.[47] In this

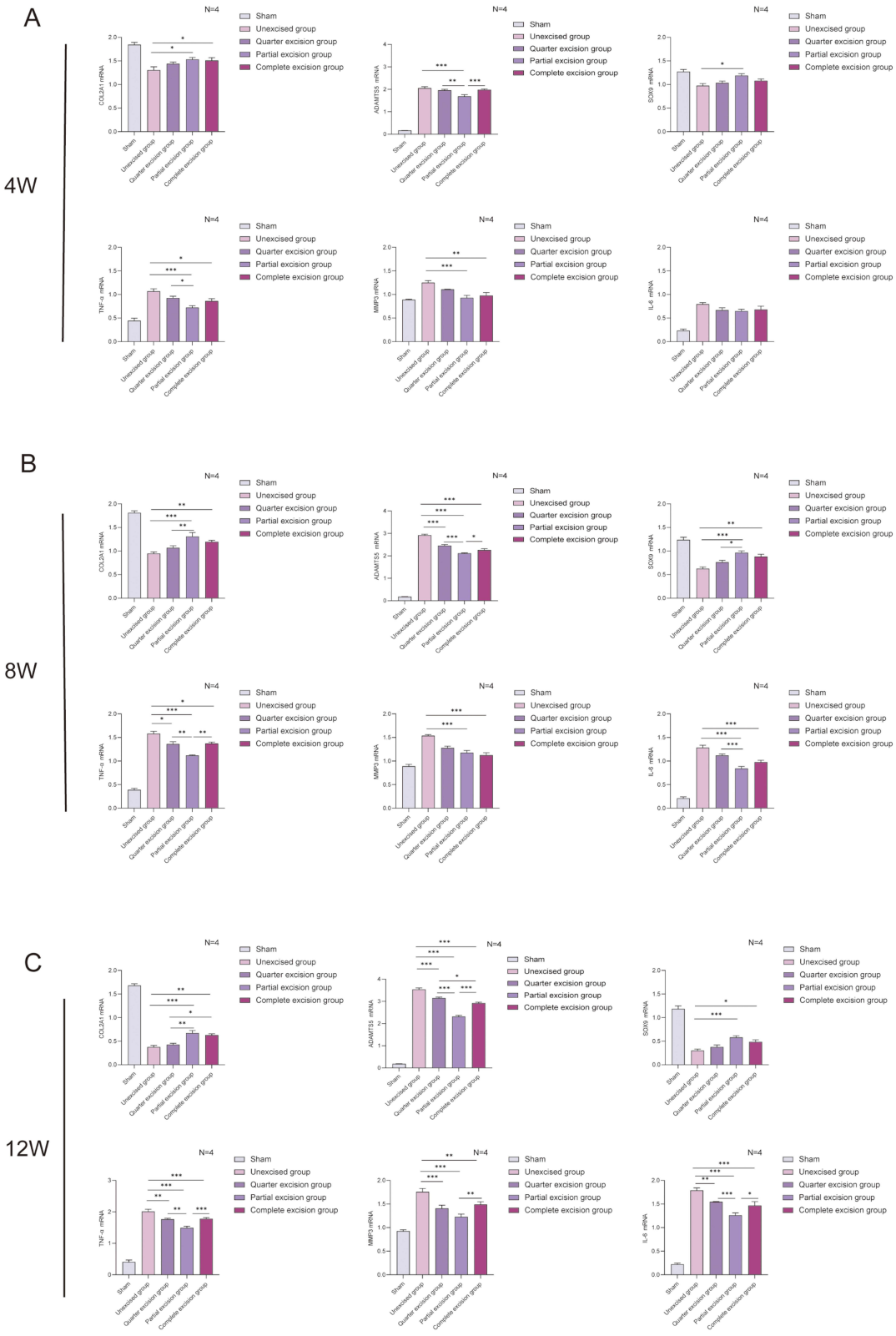

Figure 7 qRT-PCR quantitative analysis results of mouse cartilage tissue: (**A**) Expression levels of COL2A1, ADAMTS5, SOX9, TNF-α, MMP3, and IL-6 mRNA in cartilage tissue of mice at the 4 weeks. (**B**) Expression levels of COL2A1, ADAMTS5, SOX9, TNF-α, MMP3, and IL-6 mRNA in cartilage tissue of mice at the 8 weeks. (**C**) Expression levels of COL2A1, ADAMTS5, SOX9, TNF-α, MMP3, and IL-6 mRNA in cartilage tissue of mice at the 12 weeks. N=4. All the data in the bar graph are presented as mean ± S.E.M, among which *P < 0.05, **P < 0.01, and ***P < 0.001.

study, we employed micro-CT, HE staining, Safranin O-Fast Green staining, and qRT-PCR to evaluate the impact of different IFP excision methods on joint structure in the KOA mouse model.

Micro-CT analysis assessed key parameters, including Tb.N, BV/TV, Tb.Sp, and Tb.Th. At 4 weeks, no significant differences were observed among the groups for these parameters. However, as the disease progressed, particularly at 8 and 12 weeks, the partial excision group exhibited significant improvements in Tb.N, BV/TV, Tb.Sp, and Tb.Th, indicating recovery of trabecular structure, increased bone density, and enhanced bone strength compared to the unexcision group. The complete excision group also showed some improvement, although less pronounced than that seen in the partial excision group. In contrast, the quarter excision group demonstrated no significant changes, suggesting limited bone-protective effects of this approach.

HE and Safranin O-Fast Green staining revealed that the partial excision group maintained a more preserved cartilage morphology, with smooth articular surfaces and minimal signs of degeneration. In contrast, the complete excision group exhibited varying degrees of cartilage degeneration, characterized by irregular surfaces and areas of cartilage loss. The quarter excision group showed cartilage degradation similar to that of the unexcision group, with no significant improvement. Safranin O-Fast Green staining further confirmed the superior cartilage protection in the partial excision group, as evidenced by increased staining intensity, indicating better preservation of the cartilage matrix compared to the other groups.

According to the OARSI scoring system, at 4, 8, and 12 weeks, the partial excision and complete excision groups exhibited significantly less cartilage damage compared to the unexcision and quarter excision groups. This suggests that both partial and complete excision effectively reduce joint inflammation and preserve cartilage integrity, thereby slowing the progression of KOA. The quarter excision group showed no significant difference in OARSI scores compared to the unexcision group, further highlighting the superior effectiveness of partial and complete excision in protecting joint structure.

COL-2, IL-6, MMP-3, and *TNF-α* were selected as key indicators in immunohistochemical experiments to assess cartilage damage, inflammation, and matrix degradation in the KOA mouse model. *COL-2* reflects cartilage degeneration,[48] IL-6 is a pro-inflammatory cytokine linked to joint inflammation,[49] *MMP-3* is involved in matrix degradation and cartilage breakdown,[50] and *TNF-α* promotes joint damage through inflammation and apoptosis.[51] Together, these markers provide valuable insights into the pathological progression of KOA and potential therapeutic strategies.

Immunohistochemistry analysis showed significantly lower levels of inflammatory markers (such as *IL-6, TNF-α*, and *MMP-3*) in the partial excision group compared to the other three groups, indicating effective suppression of local joint inflammation. Furthermore, both the complete excision and quarter excision groups showed significant improvements in inflammatory marker expression in the mid- and late stages, relative to the unexcision group. This suggests that these two excision methods also have a notable effect in alleviating joint inflammation. These findings further highlight the crucial role of partial excision in reducing joint inflammation and inhibiting the release of inflammatory cytokines, while also indicating that both quarter excision and complete excision may modulate local immune responses, potentially slowing the progression of KOA.

The primers for *COL2A1, ADAMTS5, SOX9, TNF-α, MMP3*, and *IL-6* in qRT-PCR analysis of KOA mouse knee joint cartilage tissue were selected to reflect key processes in cartilage synthesis, degradation, and inflammation. *COL2A1* indicates cartilage synthesis, with reduced expression linked to degeneration.[52] *ADAMTS5* plays a role in cartilage matrix breakdown,[53] while *SOX9* is crucial for cartilage repair.[54] *TNF-α* and *IL-6* are pro-inflammatory cytokines that exacerbate inflammation and cartilage degradation,[50,55] and *MMP3* is involved in extracellular matrix degradation.[56]

qRT-PCR analysis revealed further differences in gene expression across the groups. Specifically, at both 8 and 12 weeks, the partial excision group exhibited significantly higher expression of cartilage-protective genes, such as *COL2A1* and Aggrecan, as well as anti-inflammatory factors like *IL-10*, compared to the complete excision and quarter excision groups. *COL2A1* and Aggrecan, key components of the cartilage matrix, were upregulated in the partial excision group, suggesting that this group effectively promoted cartilage repair and protection. Furthermore, the increased expression of *IL-10*, an anti-inflammatory cytokine, reflects the partial excision group's ability to modulate local inflammation and improve the joint environment. Collectively, these results suggest that partial excision not only mitigates inflammation but also promotes cartilage repair and inhibits the release of destructive factors, thereby contributing to the preservation of joint integrity.

The novelty of this study lies in the comprehensive application of various techniques, including gait analysis, micro-CT, HE staining, Safranin O-Fast Green staining, OARSI scoring, immunohistochemistry, and qRT-PCR, to assess the therapeutic effects of different IFP excision methods on KOA in mice. Gait analysis allowed us to dynamically monitor changes in joint stability and motor function in KOA mice, while micro-CT provided quantitative insights into bone changes.[57] HE and Safranin O-Fast Green staining further facilitated the observation of morphological alterations in cartilage. The OARSI scoring system offered both qualitative and quantitative assessments of joint damage, and immunohistochemistry and qRT-PCR revealed the molecular mechanisms underlying the effects of IFP excision on inflammation and cartilage protection.[58,59] Compared to previous studies, this research not only systematically evaluated the effects of different excision methods on joint stability, bone changes, and cartilage protection but also explored the potential of IFP excision in alleviating joint inflammation from an immunological perspective, filling a significant gap in the field.

While previous research has predominantly focused on the complete excision of the IFP, this study expands the scope by investigating the effects of both partial and quarter IFP excision in addition to complete excision. The novelty of this work lies in its investigation of how different extents of IFP removal impact the inflammatory progression of KOA while aiming to preserve as much of the IFP's normal physiological function as possible. By comparing these three excision strategies—complete, partial, and quarter excision—this study provides valuable insights into the balance between reducing inflammation and maintaining IFP functionality. These findings are crucial for identifying an optimal excision approach that minimizes inflammatory progression in KOA without compromising the IFP's critical roles in joint homeostasis, offering a potential therapeutic strategy for managing KOA.

Our study found that partial excision of the IFP significantly improved the progression of KOA, aligning with previous animal studies, such as one in guinea pigs, where early IFP excision altered disease progression.[18] Clinical studies also support these findings, showing that partial IFP excision can alleviate pain and functional impairment in KOA patients.[60] However, some studies have raised concerns about adverse effects like patellar tendon shortening following IFP excision, which may impact knee function.[61] In contrast, our partial excision approach did not significantly affect joint stability, likely due to the preservation of some IFP structure. Additionally, other non-surgical treatments targeting the IFP, such as low-intensity pulsed ultrasound (LIPUS), have also shown promise in improving KOA symptoms,[62] further supporting the IFP as a therapeutic target in managing KOA.

The partial excision group exhibited the most significant improvement in inflammation reduction. This could be due to several factors: first, the partial excision may help maintain sufficient IFP function to support joint homeostasis while reducing excessive inflammation. Second, partial excision might promote a more balanced inflammatory response, preserving the protective and anti-inflammatory properties of the IFP while limiting its contribution to KOA progression. Third, the partial removal of the IFP could reduce mechanical stress or other factors that exacerbate inflammation, without entirely eliminating the fat pad's beneficial roles in joint stability and tissue repair. This combination of factors may explain the superior anti-inflammatory effects observed in the partial excision group compared to other groups.

The experimental results from the quarter excision group did not perform as expected, and in fact, were less effective than the complete excision group. This could be due to several reasons: first, the extent of the quarter excision may have been too small to effectively reduce inflammation or alleviate joint degeneration. Given that the IFP in mice is already quite small, the reduced excision may not have achieved the desired effect. Second, the remaining portion of the IFP may still play a negative role in the joint, preventing a significant reduction in inflammation. Lastly, the effects of quarter excision could be influenced by the local physiological environment and tissue repair processes, which may not have been sufficient to significantly slow down the progression of inflammation.

Another innovative aspect of this study is its exploration of the inflammatory progression of KOA at different stages of the disease. Previous studies have largely focused on the effects of IFP excision in a single stage of KOA, but this research extends the analysis to early, middle, and late stages of KOA. By examining the inflammatory response at these different time points, the study provides a more comprehensive understanding of how IFP excision—whether complete, partial, or quarter—affects the trajectory of inflammation throughout the progression of KOA. The inclusion of multiple stages allows for a nuanced perspective on how the timing and extent of IFP excision influence the progression of joint inflammation, helping to identify the most effective intervention strategy for each stage of the disease. This approach not only enhances our understanding of the pathophysiology of KOA but also provides valuable insights for tailoring therapeutic interventions based on the stage of disease.

Although this study comprehensively analyzed the impact of IFP excision on the inflammatory progression of KOA in a murine model, there are still some limitations. First, while the mouse model is widely used in KOA research, it may not fully replicate the pathological features observed in humans. Therefore, future studies should validate these findings using clinical data or more refined animal models to enhance their clinical relevance. Second, although this study highlights the potential of different IFP excision methods in alleviating joint inflammation and protecting cartilage, the long-term effects of IFP excision remain insufficiently explored. Future research should extend the experimental duration to evaluate the efficacy of these excision protocols in the long-term progression of KOA and examine whether they might induce any potential side effects.

Additionally, while the partial excision protocol demonstrated promising therapeutic effects in the KOA mouse model, its clinical feasibility and application require further investigation. Therefore, future studies should incorporate preclinical studies, clinical trials, and analyses of human samples to assess the actual therapeutic effects and the underlying molecular mechanisms of IFP excision in KOA treatment. Moreover, combining IFP excision with other therapeutic modalities, such as pharmacological and physical treatments, may further enhance treatment outcomes, delay disease progression, and improve patients' quality of life. Future research should focus on exploring the synergistic effects of IFP excision in conjunction with other therapeutic approaches to develop more comprehensive and refined treatment strategies.

Conclusions

In this study, we investigated the effects of IFP excision, including the extent of excision, on the inflammatory progression of KOA in a murine model. Our results demonstrate that IFP excision, particularly partial and complete excision, significantly alleviates inflammation and cartilage degeneration in KOA. Step gait analysis, micro-CT imaging, and histological assessments revealed that IFP excision improves joint stability, preserves subchondral bone integrity, and reduces cartilage erosion. Moreover, immunohistochemical analysis showed a marked reduction in inflammatory markers (*IL-6, TNF-α, MMP-3*) and improved preservation of *COL-2*, most notably in the partial and complete excision groups. qRT-PCR validation further confirmed these findings at the molecular level. Collectively, these results suggest that IFP excision may represent a promising therapeutic approach for mitigating inflammation and slowing the progression of KOA, with partial excision yielding the most favorable outcomes. However, further studies are required to fully elucidate the underlying molecular mechanisms and to explore the clinical potential of IFP excision in the management of KOA.

Data Sharing Statement

The datasets used and/or analyzed during the current study are available from the corresponding authors, Rende Ning, upon reasonable request.

Ethics Approval and Consent to Participate

Ethical approval for our study was granted by The Committee on Medical Ethics of The Third Affiliated Hospital of Anhui Medical University (Reference number grant ID: 2023-021-01) and the Animal Ethics Committee of Anhui Medical University (Reference number grant ID: Anhui Medical University LLSC20242502).

Acknowledgments

We thank all the people who offer help for this study. Co-first authors: Ya Li, Peizhi Lu contributed equally to this paper. Co-Correspondence authors: Lingchao Kong, Rende Ning contributed equally to this paper.

Author Contributions

All authors made a significant contribution to the work reported, whether that is in the conception, study design, execution, acquisition of data, analysis and interpretation, or in all these areas; took part in drafting, revising or critically reviewing the article; gave final approval of the version to be published; have agreed on the journal to which the article has been submitted; and agree to be accountable for all aspects of the work.

Funding

This study was supported by Grants from Hefei Municipal Natural Science Foundation, the Key Project of Health Commission Applied Medical Research of Hefei (Hwk2024zd001), the Basic and Clinical Collaborative Research Promotion Initiative of the Third Affiliated Hospital of Anhui Medical University (2022sfy007), and Anhui Medical University Foundation (2023xkj109). The Health Research Project of Health Commission of Anhui Province (No. AHWJ2024Aa30021).

Disclosure

The authors declare that they have no conflicts of interest in this work.

References

1. Yvonne R, Elco E, Uwe H, et al. ER stress in ERp57 knockout knee joint chondrocytes induces osteoarthritic cartilage degradation and osteophyte formation. *Int J Mol Sci*. 2021;23(1):182. doi:10.3390/ijms23010182
2. Rebekah H, Elsa SS, Leena S, et al. The association between severity of radiographic knee OA and recurrent falls in middle and older aged adults: the osteoarthritis initiative. *J Gerontol Biol Sci Med Sci*. 2023;78(1):97–103.
3. Zhou J, Yan Y, Dong YW, et al. Characteristics and treatment of knee osteoarthritis in urban residents of Beijing, China: a community-based cross-sectional study. *Biomed Environ Sci*. 2024;37(4):418–422. doi:10.3967/bes2024.045
4. Rai MF, Sandell LJ. Inflammatory mediators: tracing links between obesity and osteoarthritis. *Crit Rev Eukaryot Gene Expr*. 2011;21(2):131–142. doi:10.1615/CritRevEukarGeneExpr.v21.i2.30
5. Alghadir AH, Khan M. Factors affecting pain and physical functions in patients with knee osteoarthritis: an observational study. *Medicine*. 2022;101(47):e31748. doi:10.1097/MD.0000000000031748
6. Du X, Liu ZY, Tao XX, et al. Research progress on the pathogenesis of knee osteoarthritis. *Orthop Surg*. 2023;15(9):2213–2224. doi:10.1111/os.13809
7. van Tunen JAC, Dell'Isola A, Juhl C, et al. Association of malalignment, muscular dysfunction, proprioception, laxity and abnormal joint loading with tibiofemoral knee osteoarthritis - a systematic review and meta-analysis. *BMC Musculoskelet Disord*. 2018;19(1):273. doi:10.1186/s12891-018-2202-8
8. Zeng N, Yan ZP, Chen XY, Ni GX. Infrapatellar fat pad and knee osteoarthritis. *Aging Dis*. 2020;11(5):1317–1328. doi:10.14336/AD.2019.1116
9. Madry H, Luyten FP, Facchini A. Biological aspects of early osteoarthritis. *Knee Surg Sports Traumatol Arthrosc*. 2012;20(3):407–422. doi:10.1007/s00167-011-1705-8
10. Fontanella CG, Belluzzi E, Pozzuoli A, et al. Exploring anatomo-morphometric characteristics of infrapatellar, suprapatellar fat pad, and knee ligaments in osteoarthritis compared to post-traumatic lesions. *Biomed*. 2022;10(6):6. doi:10.3390/biomedicines10061369
11. Chaofan Z, Zeyu Z, Yunzhi L, et al. A novel infrapatellar fat pad preservation technique in total knee arthroplasty reduced postoperative pain and wound complications. *Orthopaedic Surg*. 2024;16(8):1946–1954. doi:10.1111/os.14137
12. Fontanella CG, Macchi V, Porzionato A, et al. A numerical investigation of the infrapatellar fat pad. *Proc Inst Mech Eng H*. 2020;234(10):1113–1121. doi:10.1177/0954411920940839
13. Fontanella CG, Carniel EL, Frigo A, et al. Investigation of biomechanical response of Hoffa's fat pad and comparative characterization. *J Mech Behav Biomed Mater*. 2017;67:1–9. doi:10.1016/j.jmbbm.2016.11.024
14. Eymard F, Pigenet A, Citadelle D, et al. Induction of an inflammatory and prodegradative phenotype in autologous fibroblast-like synoviocytes by the infrapatellar fat pad from patients with knee osteoarthritis. *Arthritis Rheumatol*. 2014;66(8):2165–2174. doi:10.1002/art.38657
15. Fontanella CG, Belluzzi E, Pozzuoli A, et al. Mechanical behavior of infrapatellar fat pad of patients affected by osteoarthritis. *J Biomech*. 2022;131:110931. doi:10.1016/j.jbiomech.2021.110931
16. Eymard F, Chevalier X. Inflam mation of the infrapatellar fat pad. *Joint Bone Spine*. 2016;83(4):389–393. doi:10.1016/j.jbspin.2016.02.016
17. Klein-Wieringa IR, Kloppenburg M, Bastiaansen-Jenniskens YM, et al. The infrapatellar fat pad of patients with osteoarthritis has an inflammatory phenotype. *Ann Rheum Dis*. 2011;70(5):851–857. doi:10.1136/ard.2010.140046
18. Afzali MF, Radakovich LB, Sykes MM, et al. Early removal of the infrapatellar fat pad/synovium complex beneficially alters the pathogenesis of moderate stage idiopathic knee osteoarthritis in male Dunkin Hartley Guinea pigs. *Arthritis Res Ther*. 2022;24(1):282. doi:10.1186/s13075-022-02971-y
19. Bohnsack M, Wilharm A, Hurschler C, Rühmann O, Stukenborg-Colsman C, Wirth CJ. Biomechanical and kinematic influences of a total infrapatellar fat pad resection on the knee. *Am J Sports Med*. 2004;32(8):1873–1880. doi:10.1177/0363546504263946
20. Hang F, Lisi H, Ian W, et al. Early changes of articular cartilage and subchondral bone in the DMM mouse model of osteoarthritis. *Sci Rep*. 2018;8(1):2855. doi:10.1038/s41598-018-21184-5
21. Gang L, Guoyou W, Shijie F, Xiaoguang G, Xin Z, Lei Z. A Macaca fascicularis knee osteoarthritis model developed by modified hulth combined with joint scratches. *Med Sci Monit*. 2018;24:3393.
22. Wang S, Zhou J. Gait analysis of knee joint walking based on image processing. *Curr Med Imaging*. 2024;20:e15734056277482. doi:10.2174/0115734056277482240329050639
23. Bernhard V, Hanno W. Heterogeneity of animal experiments and how to deal with it. *Lab Anim*. 2024;58(5):493–497.
24. Jean-Loup R, Alan L, Lauren H, et al. Wireless 'under the skull' epidural EEG and behavior in piglets during nitrous oxide or carbon dioxide gas euthanasia. *Physiol Behav*. 2020;227:113142. doi:10.1016/j.physbeh.2020.113142
25. Zhongmin L, Clara W, Andreas R, Yi-Li C, Kristin A, Goetz M. Hypertonic saline- and detergent-accelerated EDTA-based decalcification better preserves mRNA of bones. *Sci Rep*. 2024;14(1):1. doi:10.1038/s41598-023-50600-8

26. Han X, Cui J, Xie K, et al. Osteoarthritis disease severity, and subchondral trabecular bone microarchitecture in patients with knee osteoarthritis: a cross-sectional study. *Arthritis Res Therapy*. 2020;22(1):1. doi:10.1186/s13075-020-02274-0
27. Radakovich LB, Marolf AJ, Shannon JP, Pannone SC, Sherk VD, Santangelo KS. Development of a microcomputed tomography scoring system to characterize disease progression in the Hartley Guinea pig model of spontaneous osteoarthritis. *Connect Tissue Res*. 2018;59(6):523–533. doi:10.1080/03008207.2017.1409218
28. Obeidat AM, Kim SY, Burt KG, et al. A standardized approach to evaluation and reporting of synovial histopathology in two surgically induced murine models of osteoarthritis. *Osteoarthritis Cartilage*. 2024;32(10):1273–1282. doi:10.1016/j.joca.2024.05.006
29. de Haan K, Zhang Y, Zuckerman JE, et al. Deep learning-based transformation of H&E stained tissues into special stains. *Nat Commun*. 2021;12(1):4884. doi:10.1038/s41467-021-25221-2
30. Maja Carina N, Adrian H, Maximilian Christian K, Bernd G, Heinz R. Fast green FCF improves depiction of extracellular matrix in ex vivo fluorescence confocal microscopy. *Life*. 2024.
31. Hongda S, Jiawei Y, Yajun M, et al. Evaluation of cartilage degeneration using multiparametric quantitative ultrashort echo time-based MRI: an ex vivo study. *Quant Imaging Med Surg*. 2021;12(3):1738–1749.
32. Sami K, David F, Gonçalo B, et al. Assessment of whole cartilage surface damage in an osteoarthritis rat model: the Cartilage Roughness Score (CRS) utilizing microcomputed tomography. *Osteoarthritis Cartilage*. 2024.
33. Glasson SS, Chambers MG, Van Den Berg WB, Little CB. The OARSI histopathology initiative - recommendations for histological assessments of osteoarthritis in the mouse. *Osteoarthritis Cartilage*. 2010;18(3):S17–23. doi:10.1016/j.joca.2010.05.025
34. Taavi T, Siim S, Kalle K, Marina A, Andres A. Comparison of antigen retrieval methods for immunohistochemical analysis of cartilage matrix glycoproteins using cartilage intermediate layer protein 2 (CILP-2) as an example. *Methods Protoc*. 2024;7(5):67.
35. Md Shafiullah S, Kathryn F, Rose Ann GF, et al. Method for manufacture and cryopreservation of cartilage microtissues. *J Tissue Eng*. 2023;14.
36. Bo-han Y, Bao-shan L, Ze-liang C, Bo-han Y, Bao-shan LIU, Ze-liang C. DNA extraction with TRIzol reagent using a silica column. *Anal Sci*. 2021;37(7):1033–1037. doi:10.2116/analsci.20P361
37. Shyam KA, Katherine BM, Claire W, Joseph DD, Susan EM. The trajectory of gait development in mice. *Brain Behavior*. 2020;10:6.
38. Gustavo de Oliveira Z, Pedro William Martins P, Tales Sambrano V, et al. Long-term heat acclimation training in mice: similar metabolic and running performance adaptations despite a lower absolute intensity than training at temperate conditions. *J Therm Biol*. 2024;119:103797. doi:10.1016/j.jtherbio.2024.103797
39. Jang S, Lee K, Ju JH. Recent updates of diagnosis, pathophysiology, and treatment on osteoarthritis of the knee. *Int J Mol Sci*. 2021;22(5):5. doi:10.3390/ijms22052619
40. Jiang P, Hu K, Jin L, Luo Z. A brief review of current treatment options for osteoarthritis including disease-modifying osteoarthritis drugs (DMOADs) and novel therapeutics. *Ann Med Surg*. 2024;86(7):4042–4048. doi:10.1097/MS9.0000000000002214
41. Filardo G, Kon E, Longo UG, et al. Non-surgical treatments for the management of early osteoarthritis. *Knee Surg Sports Traumatol Arthrosc*. 2016;24(6):1775–1785. doi:10.1007/s00167-016-4089-y
42. Ewa W, Dominik L, Jacob S, et al. Infrapatellar fat pad modulates osteoarthritis-associated cytokine and MMP expression in human articular chondrocytes. *Cells*. 2023.
43. Favero M, El-Hadi H, Belluzzi E, et al. Infrapatellar fat pad features in osteoarthritis: a histopathological and molecular study. *Rheumatology*. 2017;56(10):1784–1793. doi:10.1093/rheumatology/kex287
44. Wang MG, Seale P, Furman D. The infrapatellar fat pad in inflammaging, knee joint health, and osteoarthritis. *NPJ Aging*. 2024;10(1):34. doi:10.1038/s41514-024-00159-z
45. Tu B, Zhu Z, Lu P, et al. Proteomic and lipidomic landscape of the infrapatellar fat pad and its clinical significance in knee osteoarthritis. *Biochim Biophys Acta Mol Cell Biol Lipids*. 2024;1869(6):159513. doi:10.1016/j.bbalip.2024.159513
46. Zhou S, Maleitzke T, Geissler S, et al. Source and hub of inflammation: the infrapatellar fat pad and its interactions with articular tissues during knee osteoarthritis. *J Orthop Res*. 2022;40(7):1492–1504. doi:10.1002/jor.25347
47. Matthew SH, Julie ED, Lori Lyn P, et al. Composite quantitative knee structure metrics predict the development of accelerated knee osteoarthritis: data from the osteoarthritis initiative. *BMC Musculoskeletal Disorders*. 2020;21:1.
48. Anne-Christine H, Michel M, Damien L, et al. Cartilage biomarkers coll2-1 and coll2-1NO2 are associated with knee OA MRI features and are helpful in identifying patients at risk of disease worsening. *Cartilage*. 2021;13(1_suppl):1637S–47S.
49. Wiegertjes R, van de Loo FAJ, Blaney davidson EN. A roadmap to target interleukin-6 in osteoarthritis. *Rheumatology*. 2020;59(10):2681–2694. doi:10.1093/rheumatology/keaa248
50. Ivanova M, Georgiev T, Ivanova M, Ivanova M. Serum levels of matrix metalloproteinase-3 as a prognostic marker for progression of cartilage injury in patients with knee osteoarthritis. *Acta Reumatológica Portuguesa*. 2020;45(3):207–213.
51. Joschka W, Marie-Therese N, Thomas H, et al. TNF leads to mtDNA release and cGAS/STING-dependent interferon responses that support inflammatory arthritis. *Cell Rep*. 2021.
52. Luo Y, He Y, Reker D, et al. A novel high sensitivity type II collagen blood-based biomarker, PRO-C2, for assessment of cartilage formation. *Int J Mol Sci*. 2018;19(11):3485. doi:10.3390/ijms19113485
53. Javier -B-B, Tamas R, Marika F, et al. Extracellular matrix in heart failure: role of ADAMTS5 in proteoglycan remodeling. *Circulation*. 2021;144(25):2021–2034. doi:10.1161/CIRCULATIONAHA.121.055732
54. Qiuhui P, Yongchun Y, Qiongyu C, et al. Sox9, a key transcription factor of bone morphogenetic protein-2-induced chondrogenesis, is activated through BMP pathway and a CCAAT box in the proximal promoter. *J Cell Physiol*. 2008;217(1):228–241. doi:10.1002/jcp.21496
55. Hanjie Y, Mingxiu L, Xiaodong W, et al. Elevation of α-1,3 fucosylation promotes the binding ability of TNFR1 to TNF-α and contributes to osteoarthritic cartilage destruction and apoptosis. *Arthritis Res Therapy*. 2022;24(1):1–14.
56. Nasi S, Ea HK, So A, Busso N. Revisiting the role of interleukin-1 pathway in osteoarthritis: interleukin-1α and −1β, and NLRP3 Inflammasome are not involved in the pathological features of the murine menisectomy model of osteoarthritis. *Front Pharmacol*. 2017;8:282. doi:10.3389/fphar.2017.00282
57. Borges PDN, Forte AE, Vincent TL, Dini D, Marenzana M. Rapid, automated imaging of mouse articular cartilage by microCT for early detection of osteoarthritis and finite element modelling of joint mechanics. *Osteoarthritis Cartilage*. 2014;22(10):1419–1428.

58. Gunter K, Magali C, Klaus R, Dieter K, Henning M. Failed cartilage repair for early osteoarthritis defects: a biochemical, histological and immunohistochemical analysis of the repair tissue after treatment with marrow-stimulation techniques. *Knee Surg Sports Traumatol Arthrosc*. 2012;20(11):2315–2324. doi:10.1007/s00167-011-1853-x
59. Andreas L, Heiko S, Christoph Z, Richard K. Comparison of different methods of semiquantitative assessment and subjective scores for retropatellar articular cartilage evaluation in advancing osteoarthritis. *Ortop Traumatol Rehabil*. 2023;25(6):297–305.
60. Liu Y, Gao Q. Partial excision of infrapatellar fat pad for the treatment of knee osteoarthritis. *J Orthop Surg Res*. 2024;19(1):631. doi:10.1186/s13018-024-05114-y
61. Sheldon M. The effect of infrapatellar fat pad resection in total knee replacement on patella tendon length and functional outcomes after five years. *J Orthop Bone Disord*. 2019;3(4):1–7. doi:10.23880/jobd-16000187
62. Kitano M, Kawahata H, Okawa Y, et al. Effects of low-intensity pulsed ultrasound on the infrapatellar fat pad in knee osteoarthritis: a randomized, double blind, placebo-controlled trial. *J Phys Ther Sci*. 2023;35(3):163–169. doi:10.1589/jpts.35.163